IEEE Access
Multidisciplinary | Rapid Review | Open Access Journal

Received March 28, 2022, accepted April 7, 2022, date of publication April 11, 2022, date of current version April 15, 2022.

Digital Object Identifier 10.1109/ACCESS.2022.3166597

Decentralized Robust Active Disturbance Rejection Control of Modular Robot Manipulators: An Experimental Investigation With Emotional pHRI

XIAO PANG[1], XIAODONG MEN[2,3], BO DONG[2], AND TIANJIAO AN[2], (Student Member, IEEE)
[1]Institute of Scientific Research and Academic, Changchun Guanghua University, Changchun 130033, China
[2]Department of Control Science and Engineering, Changchun University of Technology, Changchun 130012, China
[3]Fulscience Automotive Electronics Company Ltd., Changchun 130014, China

Corresponding author: Tianjiao An (tianjiaoan@hotmail.com)

This work was supported in part by the National Natural Science Foundation of China under Grant 61773075, Grant 62173047, and Grant 61703055; and in part by the Scientific Technological Development Plan Project in Jilin Province of China under Grant 20200801056GH.

ABSTRACT This paper presents an active disturbance rejection control (ADRC) method for modular robot manipulators (MRMs) based on extended state observer (ESO), which solves the problem of trajectory tracking when modular robot manipulators facing the emotional physical human-robot interaction (pHRI). The dynamic model of MRMs is formulated via joint torque feedback (JTF) technique that is deployed for each joint module to design the model compensation controller. ESO is used to estimate the interconnected dynamic coupling (IDC) term and the interference term caused by emotional pHRI. An uncertainty decomposition-based robust control is developed to compensate the friction term. The terminal sliding mode control (TSMC) algorithm is introduced to the controller to provide faster convergence and higher precision control effect. Based on the Lyapunov theory, the tracking error is proved to be ultimately uniformly bounded (UUB). Finally, experiments demonstrate advantages of the proposed method.

INDEX TERMS Modular robot manipulators, extended state observer, terminal sliding mode, emotional pHRI, active disturbance rejection control.

I. INTRODUCTION

Modular robot manipulators (MRMs) have drawn widely attentions in robotics community since they possess better structural adaptability and flexibility than conventional robot manipulators. MRM consists standardized robotic modules, which consists of actuators, speed reducers, sensors and communication units. MRMs are always employed in dangerous and complex environments, such as space exploration, hazard survey and furthermore physical human-robot interaction (pHRI). Nowadays, pHRI has become a research hotspot in the field of robotics. Emotional pHRI can ensure that when humans produce different kinds of emotions, the robots can continue to complete predefined tasks according to the established requirements. Hence, appropriate control systems are required to guarantee the robustness and precision of MRMs in contact with pHRI.

Besides the properties of modularity and pHRI etc., for achieving high-precision robot control, some scholars develop control issues of manipulator under conditions of random delay [1], input dead zone [2], input saturation [3], visual servo [4], optimization verification [5], and micro-positioning [6], etc. Biglarbegian [7] gave an interval type-2 fuzzy controller for trajectory tracking of desired motion. Kasprzak [8] proposed motion planning for multicorporate MRM based on hierarchical search algorithms. Xu [9] gave an adaptive sliding mode control to achieve interaction control. Pham [10] proposed a robust control method. All aforementioned methods used the centralized control scheme. For practicality, the centralized control strategy is not suitable for the MRMs system because of its modularity and high complexity. Decentralized control is more suitable for MRMs system compared with centralized control strategy [11], [12].

The associate editor coordinating the review of this manuscript and approving it for publication was Yangmin Li.

The advantages of decentralized control are to simplify complexity of the MRM system and effectively improve the running speed [13]–[15].

In order to address the problems in enhancing interaction stability and robustness, lots of researches focused on investigating active disturbance rejection control (ADRC) method for nonlinear system [16], [17]. ADRC algorithm includes tracking differentiator, extended state observer (ESO) and nonlinear feedback, and it has been applied in many fields. In the field of robotics, ADRC algorithm has been applied in the control system of manipulator [18], such as Stewart platform [19] and calibration-free robotic eye-hand coordination [20]. Among them, ESO is a more effective and mature algorithm in ADRC. Huang *et al.* [21] studied a centralized controller based on ESO compensation, and carried out control simulation for a four-jointed finger. Ren *et al.* [22] proposed a model predictive control method with friction compensation based on the ESO for the trajectory tracking control problem of an omnidirectional mobile robot. However, the existing ESO-based ADRC of robot control method does not considering the pHRI. Indeed, the control torques of each robotic joint may increase significantly along with the instantaneous deviations of the feedback of joint position, velocity and torque measurements when in contact with external circumstance. In order to improve the convergence speed and the noise tolerance of dynamic systems, the sliding mode control (SMC) system [23] is introduced. Linear SMC is an insightful method for robot control, and it has been widely applied for its simple algorithm, fast response, and strong robustness [24]–[27]. However, the linear SMC cannot guarantee that the system error will converge to zero within a finite time. In order to provide faster convergence speed and higher control accuracy to compensate the disturbance term caused by the uncertain external environment, the terminal sliding mode control (TSMC) is designed to reach the nonlinear sliding surface [28]–[30] instantly. At the same time, JTF technique can reduce the effect of uncertain contact force created between the end-effector and payloads. Schaffer *et al.* [31] gave a perspective control method for flexible manipulators. A JTF-based distributed control method for MRMs is proposed in [32]. However, the above JTF-based robot studies did not consider the pHRI tasks. Therefore, an ideal controller for MRMs based on JTF technique should guarantee the robustness of robotic systems and the ADRC when MRMs facing the external environment.

A novel decentralized robust ADRC control is proposed for MRMs in contact with emotional pHRI. First, the dynamic model of the MRM systems is formulated via JTF technique, and the robust TSMC as well as the ADRC is developed by effectively utilizing the local dynamic information in joint space. Second, based on the uncertainty decomposition scheme, a decentralized robust controller is proposed to deal with the friction model uncertainties. Then, the ESO eliminates the effect of IDC term and interference items caused by emotional pHRI. In addition, TSMC is applied for its faster convergence and higher precision control. The experimental results directly demonstrate the effectiveness of the control algorithm. The joint position errors and velocity errors are proved to be uniformly ultimately bounded (UUB). Finally, experiments demonstrate advantages of the proposed method.

The major contributions are summarized:

1.To the best of author's knowledge, it is first time to solve decentralized robust ADRC problem of MRMs with pHRI.

2.Because of different kinds of emotion, we propose a control algorithm to meet the trajectory tracking problem of people in different emotions, and the tracking performance of MRM system can be improved by experimental verification.

II. DYNAMIC MODEL FORMULATION

A. DYNAMIC MODEL FORMULATION

Since MRMs have many mechanical modules, we formulate the MRM subsystem dynamic model (see Fig. 1). Similarly in [28], we assume following conditions.

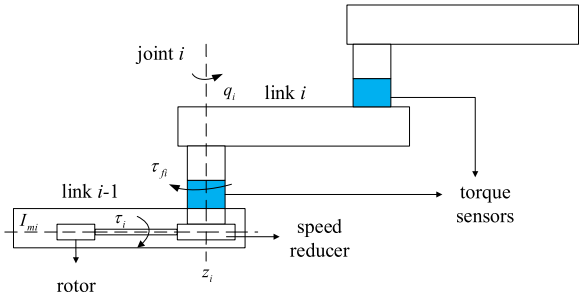

FIGURE 1. Schematic of joint module.

Assumption 1: There is no loss of torque transmission at the location of reducer.

Based on MRMs with n modules via interconnected subsystems, the ith subsystem of MRMs is [33]:

$$I_{mi}\gamma_i\ddot{q}_i + f_i(q_i,\dot{q}_i) + I_{mi}\sum_{j=1}^{i-1} z_{mi}^T z_{qj}\ddot{q}_j + \frac{\tau_{fi}}{\gamma_i} + I_{mi}\sum_{j=2}^{i-1}\sum_{k=1}^{j-1} z_{mi}^T\left(z_{qk}\times z_{qj}\right)\dot{q}_k\dot{q}_j + d_i(q_i) = \tau_i, \tag{1}$$

$I_{mi}\sum_{j=1}^{i-1} z_{mi}^T z_{qj}\ddot{q}_j + I_{mi}\sum_{j=2}^{i-1}\sum_{k=1}^{j-1} z_{mi}^T\left(z_{qk}\times z_{qj}\right)\dot{q}_k\dot{q}_j$ is the IDC, $f_i(q_i,\dot{q}_i)$ is the joint friction, z_{mi} and z_{qj} represent the unity vectors along axis of rotation of ith rotor and joint, τ_{fi}/γ_i is the coupling torque divided by gear ratio, $d_i(q_i)$ is disturbance because of uncertain environments. $d_i(q_i)$ denotes:

$$d_i(q_i) = d_{is}(q_i) + d_{ic}(q_i), \tag{2}$$

where $d_{ic}(q_i)$ is torque sensor output disturbance. $d_{is}(q_i)$ indicates external disturbance which caused by emotional pHRI.

Remark 1: The external disturbance which caused by pHRI $d_{is}(q_i)$ will change with the human's mood. When human beings are in a delighted mood, they will produce friendly actions to the robot, such as shaking hands, gently stroke, etc. When in anger or sadness emotion, humans will beat or collide with the robotic manipulator [34]–[36].

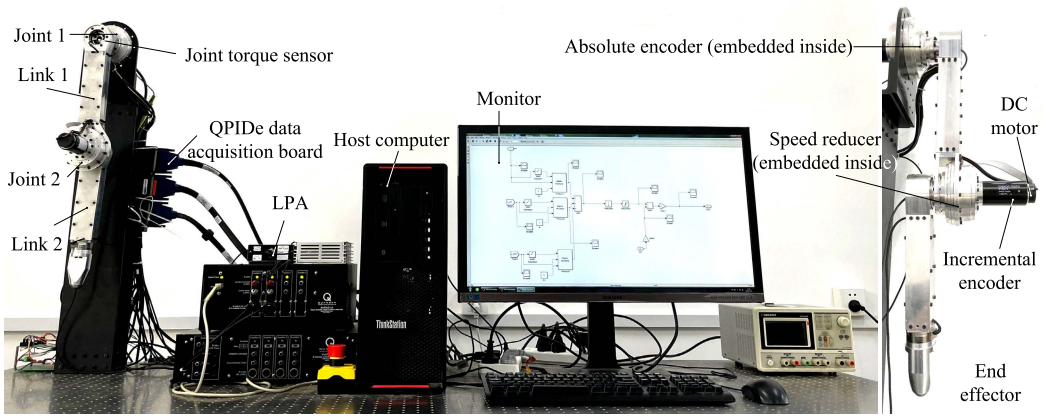

FIGURE 2. Experimental platform.

According to the reference in [37], $f_i(q_i, \dot{q}_i)$ denotes:

$$f_i(q_i, \dot{q}_i) = b_{fi}\dot{q}_i + \left(f_{ci} + f_{si}e^{(-f_{\tau i}\dot{q}_i^2)}\right) sgn(\dot{q}_i) + f_{qi}(q_i, \dot{q}_i), \quad (3)$$

where f_{ci} is Coulomb friction, f_{si} is static friction, $f_{\tau i}$ means Stribeck effect, b_{fi} is viscous friction, $f_{qi}(q_i, \dot{q}_i)$ denotes other friction errors.

We consider $f_{si}, f_{\tau i}$ are approximate to actual values, and $f_{si}e^{(-f_{\tau i}\dot{q}_i^2)}$ can be linearized as $\hat{f}_{si}, \hat{f}_{\tau i}$. Hence, we have

$$\begin{aligned} f_{si}e^{(-f_{\tau i}\dot{q}_i^2)} &= (\hat{f}_{si} + \tilde{f}_{si})(e^{(-\hat{f}_{\tau i}\dot{q}_i^2)} - \dot{q}_i^2\tilde{f}_{\tau i}e^{(-\hat{f}_{\tau i}\dot{q}_i^2)}) \\ &\approx \hat{f}_{si}e^{(-\hat{f}_{\tau i}\dot{q}_i^2)} + \tilde{f}_{si}e^{(-\hat{f}_{\tau i}\dot{q}_i^2)} - \dot{q}_i^2\tilde{f}_{\tau i}\hat{f}_{si}e^{(-\hat{f}_{\tau i}\dot{q}_i^2)}. \end{aligned} \quad (4)$$

Substituting (4) into (3), we have:

$$\begin{aligned} f_i(q_i, \dot{q}_i) \approx \hat{b}_{fi}\dot{q}_i + \left(\hat{f}_{ci} + \hat{f}_{si}e^{(\hat{f}_{\tau i}\dot{q}_i^2)}\right) sgn(\dot{q}_i) \\ + f_{qi}(q_i, \dot{q}_i) + Y(\dot{q}_i)\tilde{F}_i, \end{aligned} \quad (5)$$

where $\tilde{F}_i = [b_{fi} - \hat{b}_{fi}f_{ci} - \hat{f}_{ci}f_{si} - \hat{f}_{si}f_{\tau i} - \hat{f}_{\tau i}]^T$ indicates friction parametric uncertainty, $\hat{b}_{fi}, \hat{f}_{ci}, \hat{f}_{si}$ and $\hat{f}_{\tau i}$ denote estimated values of friction parameters, the vector is $Y(\dot{q}_i)$ regarded as

$$Y(\dot{q}_i) = \left[\dot{q}_i, sgn(\dot{q}_i), e^{(-\hat{f}_{\tau i}\dot{q}_i)}sgn(\dot{q}_i), f_{si}\dot{q}_i^2e^{(-\hat{f}_{\tau i}\dot{q}_i)}sgn(\dot{q}_i)\right]. \quad (6)$$

Rewrite the terms $I_{mi}\sum_{j=2}^{i-1}\sum_{k=1}^{j-1} z_{mi}^T\left(z_{qk} \times z_{qj}\right)\dot{q}_k\dot{q}_j$ and $I_{mi}\sum_{j=1}^{i-1} z_{mi}^T z_{qj}\ddot{q}_j$ for facilitating as follows:

$$\begin{aligned} & I_{mi}\sum_{j=1}^{i-1} z_{mi}^T z_{qj}\ddot{q}_j \\ &= I_{mi}\sum_{j=1}^{i-1} D_j^i\ddot{q}_j \\ &= \sum_{j=1}^{i-1}\left[I_{mi}\hat{D}_j^i \; I_{mi}\right]\left[\ddot{q}_j \; \tilde{D}_j^i\ddot{q}_j\right]^T = \sum_{j=1}^{i-1} I_j{}^i U_j^i, \end{aligned} \quad (7)$$

$$\begin{aligned} & I_{mi}\sum_{j=2}^{i-1}\sum_{k=1}^{j-1} z_{mi}^T\left(z_{qk} \times z_{qj}\right)\dot{q}_k\dot{q}_j \\ &= I_{mi}\sum_{j=2}^{i-1}\sum_{k=1}^{j-1}\Theta_{kj}^i\dot{q}_k\dot{q}_j \\ &= \sum_{j=2}^{i-1}\sum_{k=1}^{j-1}\left[I_{mi}\hat{\Theta}_{kj}^i \; I_{mi}\right]\left[\dot{q}_k\dot{q}_j \; \tilde{\Theta}_{kj}^i\dot{q}_k\dot{q}_j\right]^T \\ &= \sum_{j=2}^{i-1}\sum_{k=1}^{j-1} J_{kj}{}^i V_{kj}^i. \end{aligned} \quad (8)$$

We obtain relationships of $D_j^i = z_{mi}^T z_{qj}$ and $\hat{D}_j^i = D_j^i - \tilde{D}_j^i$ in (7) and (8), where D_j^i is dot product of z_{mi}, z_{qj} and $\tilde{D}_j^i$ is alignment error. We also have $\Theta_{kj}^i = z_{mi}^T\left(z_{qk} \times z_{qj}\right)$, $\hat{\Theta}_{kj}^i = \Theta_{kj}^i - \tilde{\Theta}_{kj}^i$, where Θ_{kj}^i is dot product of z_{mi}, $z_{qk} \times z_{qj}$, $\tilde{\Theta}_{kj}^i$ is alignment error. U_j^i and V_{kj}^i are model uncertainties.

Property 1: $d_{is}(q_i)$ is caused by the emotional pHRI. The term $d_{is}(q_i)$ is bounded, and up-bound is $|d_{is}(q_i)| \leq \rho_{di}$. The known up-bound $d_{ic}(q_i)$ is ρ_{dci}.

Property 2: For (3) and approximation (4), b_{fi}, f_{si}, f_{qi}, $f_{\tau i}$ and their estimations are bounded, $\tilde{F}_i$ is also bounded. $f_{qi}(q_i, \dot{q}_i)$ is bounded as $\left|f_{qi}(q_i, \dot{q}_i)\right| \leq \rho_{fqi}$, where ρ_{fqi} is bounded for any position $q_i, \dot{q}_i$.

B. SYSTEM STATE SPACE DESCRIPTION

Rewriting (1), we have

$$\ddot{q}_i = -B_i\begin{pmatrix} \left(\hat{f}_{ci} + \hat{f}_{si}e^{(-\hat{f}_{\tau i}\dot{q}_i^2)}\right) sgn(\dot{q}_i) + f_{qi}(q_i, \dot{q}_i) \\ + Y(\dot{q}_i)\tilde{F}_i + d_i(q_i) + \dfrac{\tau_{fi}}{\gamma_i} + \hat{b}_{fi}\dot{q}_i - \tau_i \\ + \sum_{j=2}^{i-1}\sum_{k=1}^{j-1} V_{kj}^i + \sum_{j=1}^{i-1} U_j^i \end{pmatrix}, \quad (9)$$

where $B_i = (I_{mi}\gamma_i)^{-1}$. Define $x_i = \left[x_{i1} \; x_{i2}\right]^T = \left[q_i \; \dot{q}_i\right]^T$. The state space equation is

$$\begin{cases} \dot{x}_{i1} = x_{i2} \\ \dot{x}_{i2} = \phi_i(x_i) + h_i(x) + \vartheta_i(x_i) + B_i\tau_i \\ y_i = x_{i1}, \end{cases} \quad (10)$$

where $\phi_i(x_i) = -B_i(\hat{b}_{fi}x_{i2} + (\hat{f}_{ci} + \hat{f}_{si}e^{(-\hat{f}_{\tau i}x_{i2}^2)})sgn(x_{i2}) + \frac{\tau_{fi}}{\gamma_i})$ represents precise modeling and measurable part. $h_i(x) = -B_i(\sum_{j=1}^{i-1} U_j^i + \sum_{j=2}^{i-1}\sum_{k=1}^{j-1} V_{kj}^i) + d_i(x_i)$ represents IDC term and external disturbance, $\vartheta_i(x_i) = -B_i f_{qi}(x_{i1}, x_{i2})$

$-B_i Y(x_{i2})\tilde{F}_i$ represents the uncertain part of the friction modeling.

Next, a decentralized robust ADRC in contact with emotional pHRI is proposed to ensure tracking error UUB.

III. DECENTRALIZED ROBUST ADRC BASED ON TSMC

A. DESIGN OF ROBUST SLIDING MODE CONTROLLER

According to (9), we define the actuator output torque:

$$\tau_i = (\tau_{fi}/\gamma_i) + u_i, \tag{11}$$

where u_i is control input of ith joint. Define parameters:

$$e_{i1} = q_i - q_{id}, r_i = \dot{e}_{i1} + \lambda_i e_{i1}, a_i = \ddot{q}_{id} - 2\lambda_i \dot{e}_{i1} - {\lambda_i}^2 e_{i1}, \tag{12}$$

where e_{i1} is the position tracking error, r_i is the filter error term, a_i is the auxiliary error function, λ_i is arbitrary positive constant, q_{id} is the expected trajectory. Then u_i is defined as:

$$u_i = u_{ic1} + u_{ir} + u_{in3}, \tag{13}$$

where $u_{ic1} = I_{mi}\gamma_i a_i + \hat{b}_i \dot{q}_i + \left(\hat{f}_{ci} + \hat{f}_{si} e^{(-\hat{f}_{\tau i}\dot{q}_i^2)}\right) sgn(\dot{q}_i)$ compensates for the moment of motor. u_{ir} is a robust controller to deal with friction modeling. u_{in3} is active disturbance rejection controller, which compensates IDC and disturbance torque item $d_i(q_i)$.

Therefore, the decentralized robust ADRC problem has transformed obtaining u_{ic1}, u_{ir} and u_{in3}, and in this way, to realize compensation of model uncertainty as well as emotional pHRI.

Next, we design a decentralized robust controller to compensate the model uncertainties.

First, we decompose $\tilde{F}_i$ into:

$$\tilde{F}_i = \tilde{F}_{ic} + \tilde{F}_{iv}, \tag{14}$$

where $\tilde{F}_{ic}$ is unknown constant vector, $\tilde{F}_{iv}$ is limited by:

$$\left|\tilde{F}_{iv}\right| < \rho_{in}. \tag{15}$$

Based on decentralized controller design, we choose:

$$u_{ir2} = u_u^i + Y(\dot{q}_i)(u_{pc}^i + u_{pv}^i), \tag{16}$$

where u_u^i is compensate $f_{qi}(q_i, \dot{q}_i)$. u_{pc}^i and u_{pv}^i compensate $\tilde{F}_{ic}$ and $\tilde{F}_{iv}$. The control of the ith joint u_{pc}^i, u_{pv}^i and u_u^i are defined as:

$$u_u^i = \begin{cases} -\rho_{fi}\dfrac{r_i}{|r_i|}, & |r_i| > \varepsilon^i \\ -\rho_{fi}\dfrac{r_i}{\varepsilon^i}, & |r_i| \le \varepsilon^i, \end{cases} \tag{17}$$

$$u_{pc}^i = -k\int_0^t Y(\dot{q}_1)^{\mathrm{T}} r_i d\tau, \tag{18}$$

$$u_{pv}^i = \begin{cases} -\rho_n^i \dfrac{\zeta_n^i}{|\zeta_n^i|}, & \left|\zeta_n^i\right| > \varepsilon_{pn}^i \\ -\rho_n^i \dfrac{\zeta_n^i}{\varepsilon_{pn}^i}, & \left|\zeta_n^i\right| \le \varepsilon_{pn}^i, \end{cases} \quad n = 1, 2, 3, 4, \tag{19}$$

where $\zeta^i = Y(\dot{q}_1)^{\mathrm{T}} r_i$, ε^i, ε_{pn}^i are positive control parameters.

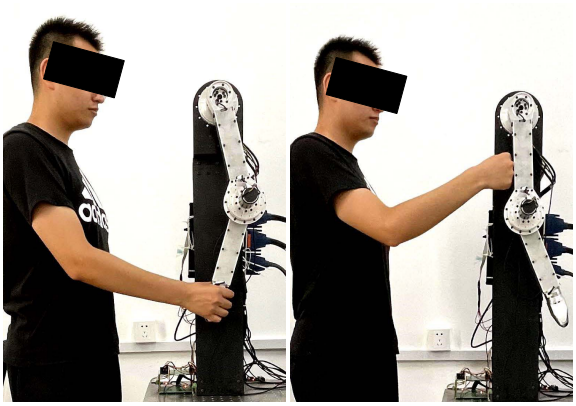

(a) (b)

FIGURE 3. Experimental condition with different emotion. (a) Delighting (b) Sadness.

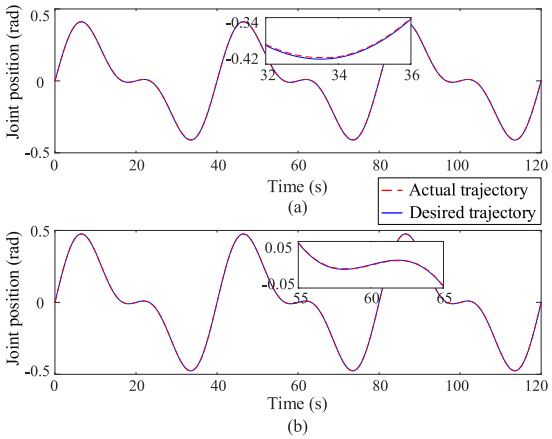

FIGURE 4. Position tracking curve via existing method under situation one. (a) Joint One (b) Joint Two.

After that, to improve the convergence rate, the TSMC algorithm is introduced in this paper, firstly, the position tracking errors of e_{i1} and e_{i2} are defined as follows:

$$\begin{cases} e_{i1} = q_i - q_{id} \\ e_{i2} = \dot{q}_i - \alpha_i, \end{cases} \tag{20}$$

where α_i denotes virtual control, and as shown follow:

$$\alpha_i = \dot{q}_{id} - \eta_i e_{i1}, \tag{21}$$

where η_i is a positive integer. The time derivative of e_{i1}, e_{i2} is taken:

$$\begin{cases} \dot{e}_{i1} = e_{i2} - \eta_i e_{i1} \\ \dot{e}_{i2} = \vartheta_i(x_i) + h_i(x) - (I_{mi}\gamma_i)^{-1}\dfrac{\tau_{fi}}{\gamma_i} \\ \qquad\qquad +(I_{mi}\gamma_i)^{-1}\tau_i - \dot{\alpha}_i. \end{cases} \tag{22}$$

Select the following Lyapunov functions for the ith subsystem:

$$V_{i1} = \frac{1}{2}e_{i1}^2. \tag{23}$$

The derivation of the above formula can be obtained:

$$\dot{V}_{i1} = e_{i1}e_{i2} - \eta_i e_{i1}^2. \tag{24}$$

For ensuring stability of SMC, the state can follow desired state within a specified finite time, and tracking error converges asymptotically to 0.

Secondly, define TSMC:

$$s_i = e_{i2} + \beta_i e_{i1}^{\frac{q_i}{p_i}-1}, \tag{25}$$

where β_i is arbitrary positive number, p_i and q_i are any positive odd numbers, and $p_i > q_i > 0$. By (22) and (23), we can obtain the derivative of s_i with respect to time:

$$\begin{aligned}\dot{s}_i &= \dot{e}_{i2} + \beta_i \frac{q_i}{p_i} e_{i1}^{\frac{q_i}{p_i}-1}\dot{e}_{i1} \\ &= \vartheta_i(x_i) + h_i(x) - (I_{mi}\gamma_i)^{-1}\frac{\tau_{fi}}{\gamma_i} - \dot{\alpha}_i \\ &\quad + (I_{mi}\gamma_i)^{-1}\tau_i + \beta_i \frac{q_i}{p_i} e_{i1}^{\frac{q_i}{p_i}-1}\dot{e}_{i1}.\end{aligned} \tag{26}$$

The decentralized sliding mode control law is:

$$u_{ir1} = \frac{\dot{\alpha}_i - \beta_i \frac{q_i}{p_i} e_{i1}^{\frac{q_i}{p_i}-1}\dot{e}_{i1} - k_i s_i - e_{i1}}{(I_{mi}\gamma_i)^{-1}} + \frac{\tau_{fi}}{\gamma_i}. \tag{27}$$

In the end, the robust sliding mode controller is:

$$\begin{aligned}u_{ir} &= u_{ir1} + u_{ir2} \\ &= u_u^i + Y(\dot{q}_i)(u_{pc}^i + u_{pv}^i) + \frac{\tau_{fi}}{\gamma_i} \\ &\quad + \frac{\dot{\alpha}_i - \beta_i \frac{q_i}{p_i} e_{i1}^{\frac{q_i}{p_i}-1}\dot{e}_{i1} - k_i s_i - e_{i1}}{(I_{mi}\gamma_i)^{-1}}.\end{aligned} \tag{28}$$

B. DESIGN OF ACTIVE DISTURBANCE REJECTION CONTROLLER

In this part, we introduce the ADRC based on the ESO. Based on the state space (10), the extended state is introduced to estimate IDC term and interference items which caused by contact with emotional pHRI.

Define the following terms for the active disturbance rejection controller design.

$$z_2 = \dot{e}_{i1} + k_1 e_{i1} = \dot{q}_i - k_1 q_{id} - x_{2eq}, x_{2eq} = \dot{q}_{id} - k_1 e_{i1}, \tag{29}$$

where k_1 is a positive feedback gain. ESO deals with modeling uncertainty in feedback linearization control [38]. First, (10) is now described as:

$$\begin{cases}\dot{x}_{i1} = x_{i2} \\ \dot{x}_{i2} = \phi_i(x_i) + \vartheta_i(x_i) + B_i u_{in3}, \\ \dot{x}_{i3} = h_i(x)\end{cases} \tag{30}$$

From (30), a linear ESO is defined as:

$$\begin{cases}\dot{\hat{x}}_{i1} = \hat{x}_{i2} - 3\omega_0(\hat{x}_{i1} - x_{i1}) \\ \dot{\hat{x}}_{i2} = \phi_i(x_i) + B_i u_{in3} + \hat{x}_{i3} + 3{\omega_0}^2(\hat{x}_{i1} - x_{i1}), \\ \dot{\hat{x}}_{i3} = -{\omega_0}^3(\hat{x}_{i1} - x_{i1})\end{cases} \tag{31}$$

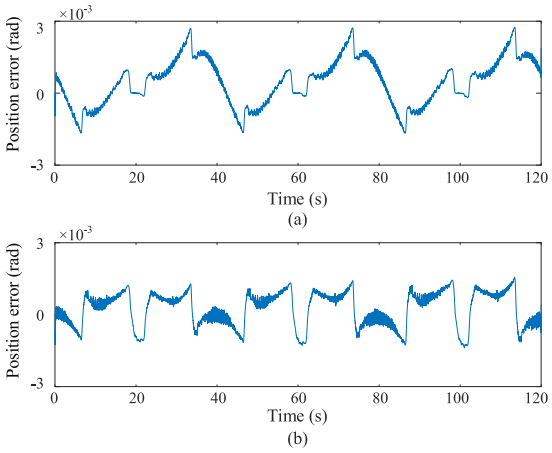

FIGURE 5. Position error curve via existing method under situation one. (a) Joint One (b) Joint Two.

where $\hat{x}_i = [\hat{x}_{i1}, \hat{x}_{i2}, \hat{x}_{i3}]^T$ is the state estimation and $\omega_0 > 0$ means the bandwidth of ESO. According to [39], we have

$$\lambda_0(s) = (s + \omega_0)^3. \tag{32}$$

Denote $\tilde{x}_{ij} = x_{ij} - \hat{x}_{ij}, j = 1, 2, 3$ as estimation error. From (31), (32), the estimation error is:

$$\begin{cases}\dot{\tilde{x}}_{i1} = \tilde{x}_{i2} - 3\omega_0\tilde{x}_{i1} \\ \dot{\tilde{x}}_{i2} = \tilde{x}_{i3} - 3{\omega_0}^2\tilde{x}_{i1} \\ \dot{\tilde{x}}_{i3} = h_i(x) - {\omega_0}^3\tilde{x}_{i1}.\end{cases} \tag{33}$$

Define $\varepsilon_{ij} = \tilde{x}_{ij}/\omega_0^{j-1}, j = 1, 2, 3$, then, (33) can be rewritten as:

$$\dot{\varepsilon}_{ij} = \omega_0 A_i \varepsilon_{ij} + M\frac{h_i(x)}{\omega_0^2}, \tag{34}$$

where A_i is Hurwitz inferred in (33) and $M = [0, 0, 1]^T$.

Lemma 1: Assuming $h_i(x)$ is bounded, estimated states are bounded and exists $\sigma_{ij} > 0$, $T_1 > 0$ such that $|\tilde{x}_{ij}| \le \sigma_{ij}$, $\sigma_{ij} = O(\frac{1}{\omega_o^c}), j = 1, 2, 3, \forall t \ge T_1$ for any positive integer c.

So that we can obtain ESO-based control law:

$$u_{in3} = (\dot{x}_{2eq} - \phi_i(x_i) - k_2 z_2 - \hat{x}_{i3})/B_i. \tag{35}$$

Combined with (11), (13), (28), and (35), the decentralized controller is:

$$\begin{aligned}\tau_i &= \frac{\tau_{fi}}{\gamma_i} + u_{ic1} + u_{ir} + u_{in3} = u_u^i - I_{mi}\gamma_i a_i + \hat{b}_i x_{i2} + \frac{\tau_{fi}}{\gamma_i} \\ &\quad + (\dot{x}_{2eq} - \phi_i(x_i) - k_2 z_2 - \hat{x}_{i3})/B_i + Y(x_{i2})(u_{pc}^i + u_{pv}^i) \\ &\quad + \left(-\dot{\alpha}_i + \beta_i \frac{q_i}{p_i} e_{i1}^{q_i/p_i - 1}\dot{e}_{i1} + k_i s_i + e_{i1}\right)/B_i \\ &\quad + \left(\hat{f}_{ci} + \hat{f}_{si} e^{(-\hat{f}_{\tau i}\dot{q}_i^2)}\right) sgn(x_{i2}).\end{aligned} \tag{36}$$

Remark 2: With the combination of the sliding mode control and active disturbance rejection control, the estimated disturbance and chattering can be observed, and then adjust the switch gain to reduce chattering effect generated by the system.

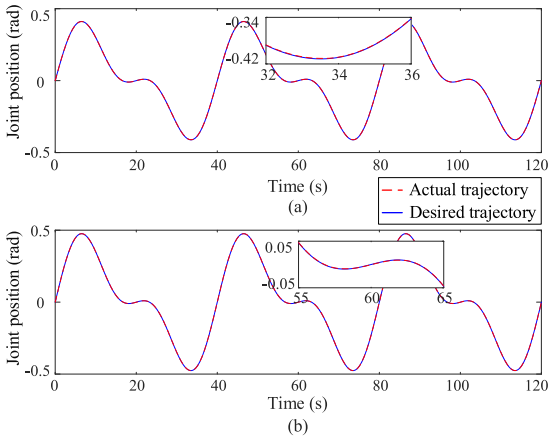

FIGURE 6. Position tracking curve via proposed method under situation one. (a) Joint One (b) Joint Two.

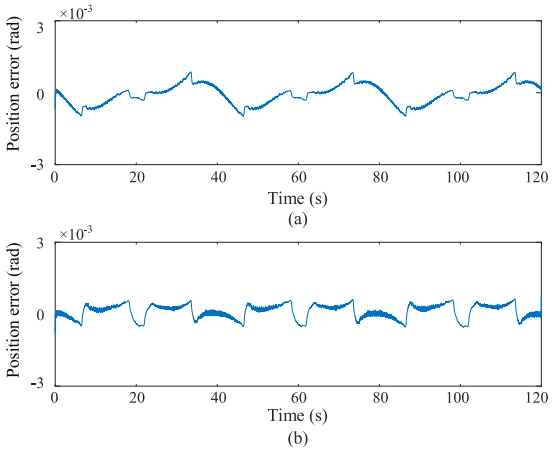

FIGURE 7. Position tracking error via proposed method under situation one. (a) Joint One (b) Joint Two.

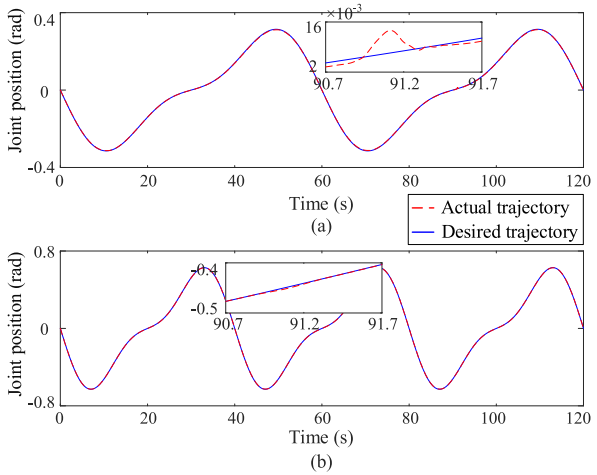

FIGURE 8. Position tracking curve via proposed method under situation two. (a) Joint One (b) Joint Two.

C. STABILITY PROOF

Theorem 1: Consider n modules MRMs system with (1), and the model uncertainty is defined by (7) and (8), as well as the disturbance term caused by the emotional pHRI in (2).

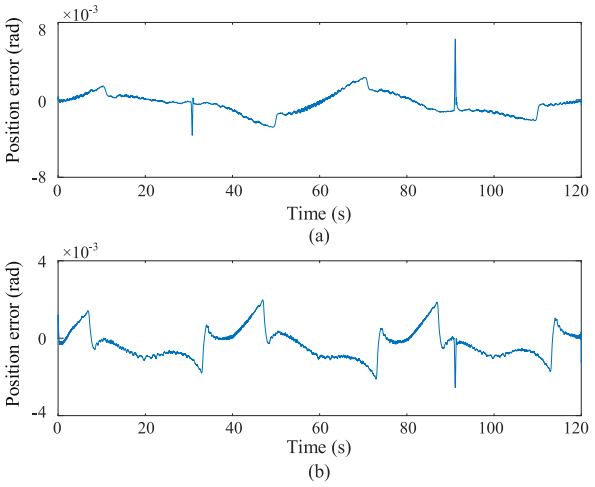

FIGURE 9. Position tracking error via proposed method under situation two. (a) Joint One (b) Joint Two.

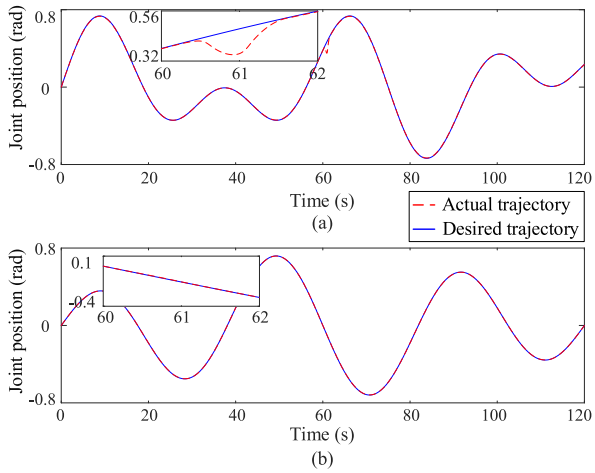

FIGURE 10. Position tracking curve via proposed method under situation three. (a) Joint One (b) Joint Two.

The tracking error can be guaranteed UUB under control law proposed by (36).

Proof: Select Lyapunov candidate function:

$$V_{i2} = \frac{1}{2}\sum_{i=1}^{n} s_i^2. \tag{37}$$

Then, the derivative of (37):

$$\dot{V}_{i2} = \sum_{i=1}^{n} s_i \dot{s}_i. \tag{38}$$

Therefore, the derivative of Lyapunov function is shown:

$$\begin{aligned}\dot{V}_i &= \sum_{i=1}^{n} (\dot{V}_{i1} + \dot{V}_{i2}) = \sum_{i=1}^{n} (e_{i1}e_{i2} - \eta_i e_{i1}^2 + s_i \dot{s}_i) \\ &= \sum_{i=1}^{n} \begin{pmatrix} s_i(\vartheta_i(x_i) + \hat{h}_i(x) - (I_{mi}\gamma_i)^{-1}\dfrac{\tau_{si}}{\gamma_i} + (I_{mi}\gamma_i)^{-1}\tau_i \\ -\dot{\alpha}_i + \beta_i \dfrac{q_i}{p_i} e_{i1}^{q_i/p_i - 1}\dot{e}_{i1}) + e_{i1}e_{i2} - \eta_i e_{i1}^2 - \dot{\alpha}_i \end{pmatrix}\end{aligned}$$

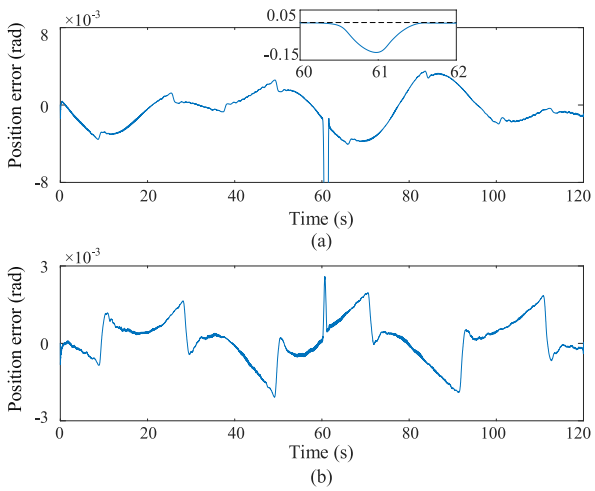

FIGURE 11. Position tracking error via proposed method under situation three. (a) Joint One (b) Joint Two.

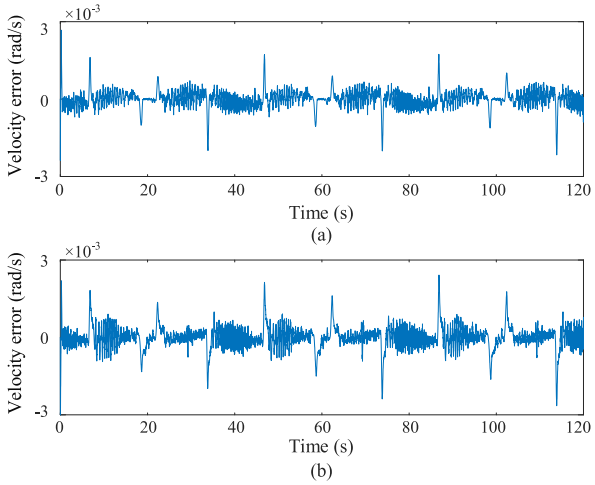

FIGURE 12. Velocity error curve via existing method under situation one. (a) Joint One (b) Joint Two.

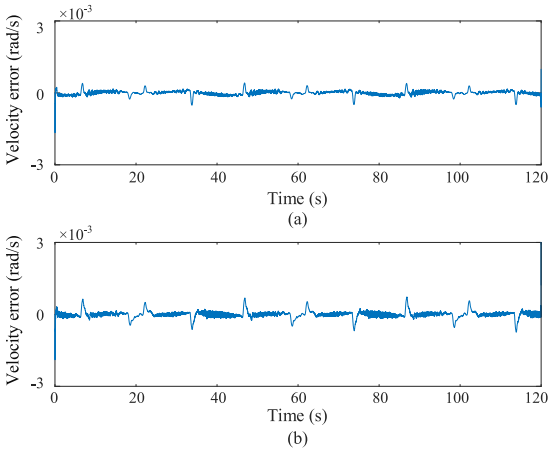

FIGURE 13. Velocity error curve via proposed method under situation one. (a) Joint One (b) Joint Two.

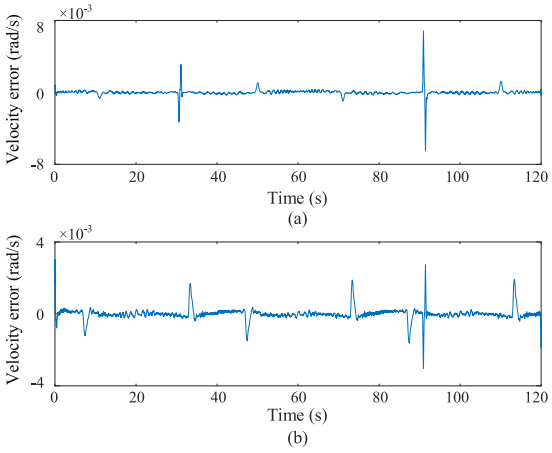

FIGURE 14. Velocity error curve via proposed method under situation two. (a) Joint One (b) Joint Two.

$$= \sum_{i=1}^{n} \left(e_{i1}e_{i2} - \eta_i e_{i1}^2 + s_i \left(\vartheta_i(x_i) + \hat{h}_i(x) - k_i s_i \right) \right). \quad (39)$$

$$\dot{V}_i \leq \sum_{i=1}^{n} (-k_i s_i^2 - \beta_i e_{i1}^{qi/pi+1} \dot{e}_{i1} - \eta_i e_{i1}^2) \leq 0. \quad (40)$$

Since $\dot{V}_i \leq 0$ is negative semidefinite, which implies s_i is bounded. Denote $V_p = \sum_{i=1}^{n} (k_i s_i^2 + \beta_i e_{i1}^{qi/pi+1} + \eta_i e_{i1}^2)$ is integrated from 0 to t, which is:

$$\int_0^t V_p d\tau \leq -\int_0^t \dot{V}_i d\tau = V(0) - V(t). \quad (41)$$

Since $V(0)$ is bounded, $V(t)$ is non-increasing with time, so that:

$$\lim_{t\to\infty} \int_0^t V_p d\tau < \infty. \quad (42)$$

According to Barbalat's lemma, $V_p(t) \to 0$ is known when $t \to \infty$ is used. It means $e_{i1} \to 0, s_i(t) \to 0$. and, if $e_{i1} = 0, s_i(t) = 0$. The tracking error of the MRMs system will asymptotically be 0, in the end the theorem is completed.

IV. EXPERIMENTS

A. EXPERIMENTAL SETUP

The platform (See Fig. 2) is composed of QPIDe data acquisition board, a linear power amplifier (LPA), two sets of joint modules and a speed reducer and an absolute encoder.

We consider two kinds of emotional pHRI which include delighting and sadness (See Fig. 3). For the first situation, the player feels happy thus shaking hands with the end-effector of the manipulator. In the second scene, the player is dissatisfied and tap the manipulator at 30s and 90s. For the third situation, people beat the manipulator to demonstrate the motion, and after a while at 60s, people shake hands with manipulator initiatively to demonstrate the apology. The robotic joints are followed with the trajectories of

$$q_{1d} = \frac{3}{10}\sin(\frac{\pi}{20})t + \frac{\pi}{18}\sin(\frac{\pi}{10})t,$$
$$q_{2d} = \frac{1}{5}\sin(\frac{\pi}{10})t + \frac{\pi}{9}\sin(\frac{\pi}{20})t,$$

TABLE 1. Parameter setting.

Parameter Type	Name	Value	Name	Value	Name	Value
Model parameter	$\hat{b}_{fi}$	12mNm/rad	$\hat{f}_{ci}$	30mNm	$\hat{f}_{si}$	40mNm
	$\hat{f}_{\tau i}$	$20s^2/rad^2$	I_{mi}	$120gcm^2$	γ_i	0.9
	ρ_{di}	5Nm	ρ_{dci}	2.5Nm	ρ_{fqi}	1
Control parameter Condition One	α_i	0.8	β_i	1.2	η_i	5
	p_i	5	q_i	3	k_i	1.2
Control parameter Condition Two	α_i	0.5	β_i	0.9	η_i	2
	p_i	7	q_i	5	k_i	1.1
Control parameter Condition Three	α_i	0.66	β_i	1.1	η_i	4
	p_i	9	q_i	7	k_i	0.8

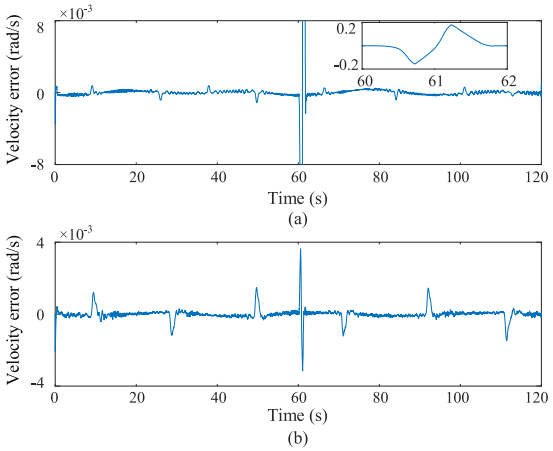

FIGURE 15. Velocity error curve via proposed method under situation three. (a) Joint One (b) Joint Two.

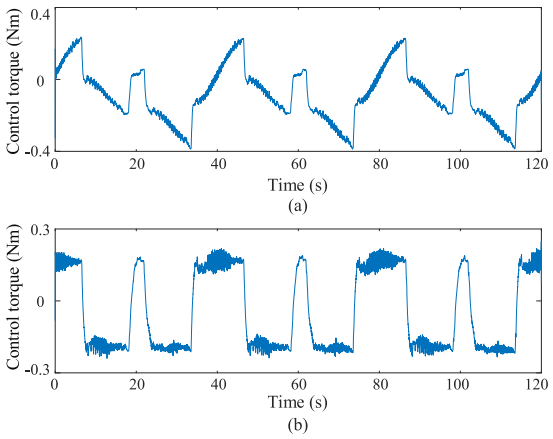

FIGURE 16. Control torque curve via existing method under situation one. (a) Joint One (b) Joint Two.

for the first situation and

$$q_{1d} = -\frac{1}{10}\sin(\frac{\pi}{15})t - \frac{\pi}{12}\sin(\frac{\pi}{30})t,$$
$$q_{2d} = -\frac{1}{5}\sin(\frac{\pi}{10})t - \frac{\pi}{6}\sin(\frac{\pi}{20})t,$$

for the second scene and the third situation is

$$q_{1d} = \frac{2}{5}\sin(\frac{\pi}{25})t + \frac{\pi}{8}\sin(\frac{\pi}{15})t,$$
$$q_{2d} = \frac{4}{5}\sin(\frac{\pi}{20})t - \frac{\pi}{10}\sin(\frac{\pi}{30})t.$$

TABLE 2. Physics parameter setting of different emotions.

Physics parameter	Delighting	Sadness	Fusion
Up-bound of disturbance torque	0.3Nm	2.2Nm	1.3Nm
Amplitude of trajectory	0.5rad	0.3rad	1.2rad
Frequency of trajectory	40/s	60/s	55/s

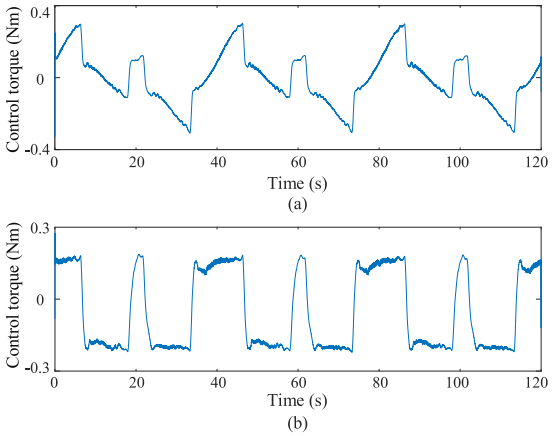

FIGURE 17. Control torque curve via proposed method under situation one. (a) Joint One (b) Joint Two.

The model parameters and control parameters of different emotion are given in Table 1. The physics parameters of various mood are shown in Table 2.

B. EXPERIMENTAL RESULTS

For comparing the advantages between existing [40]–[42] and proposed method, two different control scheme are taken into account.

1) POSITION TRACKING PERFORMANCE

Figs. 4-7 are trajectory tracking curves with delighted emotion, respectively. From these figures, both methods are effective. Figs. 8-11 are trajectory tracking and error curves with sadness and fusion emotion, respectively. We can obtain the negative emotion appear, the position trajectory can also follow the desired trajectory.

2) VELOCITY TRACKING PERFORMANCE

Figs. 12 and 13 are velocity error tracking curves under existing and proposed control methods with delighted emotion. The existing and proposed method of up-bound velocity error

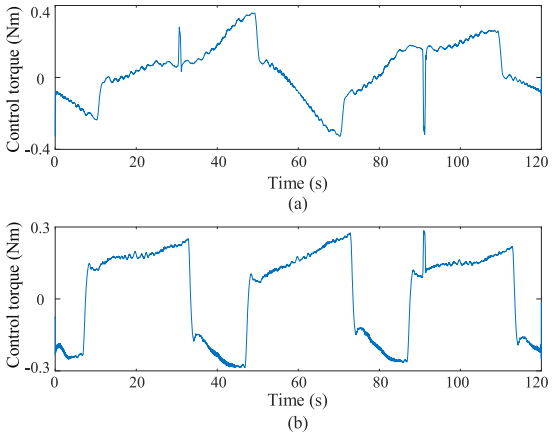

FIGURE 18. Control torque curve via proposed method under situation two. (a) Joint One (b) Joint Two.

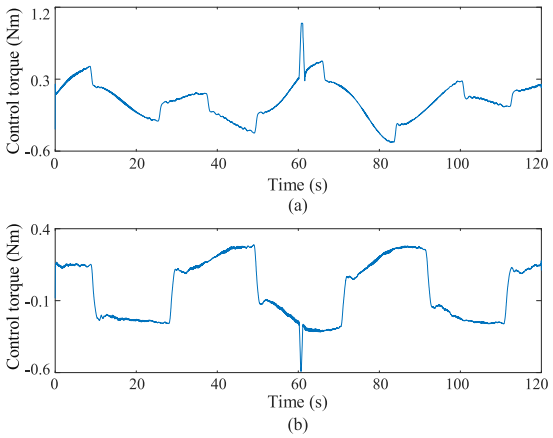

FIGURE 19. Control torque curve via proposed method under situation three. (a) Joint One (b) Joint Two.

are less than 3e-3rad/s, 1e-3rad/s. That is because the existing method has not considered ADRC to compensate the IDC effects and emotional pHRI. Fig. 14 is velocity error tracking curves under proposed control method with sadness emotion. When emotional pHRI happens, the error values decrease to normal ranges within short time, which may attribute to active disturbance rejection control. Fig. 15 is velocity error tracking curves under proposed control method with fusion emotion. We can get the similar results with delighted and sadness emotion, that is attributed to the effective decentralized robust ADRC method.

3) CONTROL TORQUE

Figs. 16, 17 are control torque tracking curves via situation one of existing and proposed method. In Fig. 16, control torque curves are with serious chattering effect. Better curves are in Fig. 17, which profits from the proposed control methods. Figs. 18 and 19 are control torques under situation two and three. In the figures, we can see curves may multiply increase when emotional pHRI occurred and lead to the robotic system out of control. The proposed active disturbance rejection control realizes the optimization of tracking errors.

For the experimental results one can get the proposed ADRC method can guarantee stability as well as accuracy.

V. CONCLUSION

A decentralized ADRC scheme for MRMs in contact with emotional disturbance is proposed. Based on JTF technique, we obtain the dynamic model of MRM. When MRM systems facing external environment, we transform the control problem with emotional pHRI into active disturbance rejection. Based on the strong estimation ability of ESO, we design ADRC, and it is used to estimate IDC term and the interference term caused by emotional pHRI. TSMC is used to guarantee high precision control as well as fast convergence. According to Lyapunov method, trajectory tracking error is proved to be UUB. Experiments are performed to confirm effectiveness.

In our future work, there will be a more detailed and completed analysis of what kind of interaction behavior human will do for different emotions.

REFERENCES

[1] Z. Li, Y. Xia, and F. Sun, "Adaptive fuzzy control for multilateral cooperative teleoperation of multiple robotic manipulators under random network-induced delays," *IEEE Trans. Fuzzy Syst.*, vol. 22, no. 2, pp. 437–450, Apr. 2014.

[2] W. He, Y. Dong, and C. Sun, "Adaptive neural impedance control of a robotic manipulator with input saturation," *IEEE Trans. Syst., Man, Cybern., Syst.*, vol. 46, no. 3, pp. 334–344, 2016.

[3] W. He, A. O. David, Z. Yin, and C. Sun, "Neural network control of a robotic manipulator with input deadzone and output constraint," *IEEE Trans. Syst., Man, Cybern., Syst.*, vol. 46, no. 6, pp. 759–770, Jun. 2016.

[4] M. Sadeghzadeh, D. Calvert, and H. A. Abdullah, "Self-learning visual servoing of robot manipulator using explanation-based fuzzy neural networks and Q-learning," *J. Intell. Robotic Syst.*, vol. 78, no. 1, pp. 83–104, Apr. 2015.

[5] B. Ding, X. Li, and Y. Li, "FEA-based optimization and experimental verification of a typical flexure-based constant force module," *Sens. Actuators A, Phys.*, vol. 332, Dec. 2021, Art. no. 113083.

[6] B. Ding, Z. Yang, and Y. Li, "Design of flexure-based modular architecture micro-positioning stage," *Microsyst. Technol.*, vol. 26, no. 9, pp. 2893–2901, Sep. 2020.

[7] M. Biglarbegian, W. W. Melek, and J. M. Mendel, "Design of novel interval type-2 fuzzy controllers for modular and reconfigurable robots: Theory and experiments," *IEEE Trans. Ind. Electron.*, vol. 58, no. 4, pp. 1371–1384, Apr. 2011.

[8] W. Kasprzak, W. Szynkiewicz, D. Zlatanov, and T. Zielińska, "A hierarchical CSP search for path planning of cooperating self-reconfigurable mobile fixtures," *Eng. Appl. Artif. Intell.*, vol. 34, pp. 85–98, Sep. 2014.

[9] Q. Xu, "Adaptive discrete-time sliding mode impedance control of a piezoelectric microgripper," *IEEE Trans. Robot.*, vol. 29, no. 3, pp. 663–673, Jun. 2013.

[10] C. Van Pham and Y. N. Wang, "Robust adaptive trajectory tracking sliding mode control based on neural networks for cleaning and detecting robot manipulators," *J. Intell. Robotic Syst.*, vol. 79, no. 1, pp. 101–114, Jul. 2015.

[11] F. Angelini, C. D. Santina, M. Garabini, M. Bianchi, G. M. Gasparri, G. Grioli, M. G. Catalano, and A. Bicchi, "Decentralized trajectory tracking control for soft robots interacting with the environment," *IEEE Trans. Robot.*, vol. 34, no. 4, pp. 924–935, Aug. 2018.

[12] X. Li and M. F. Ercan, "Decentralized coordination control for a network of mobile robotic sensors," *Wireless Pers. Commun.*, vol. 102, no. 4, pp. 2429–2442, Oct. 2018.

[13] Z. Li, S. Deng, C. Su, G. Li, Z. Yu, Y. Liu, and M. Wang, "Decentralised adaptive control of cooperating robotic manipulators with disturbance observers," *IET Control Theory Appl.*, vol. 8, no. 7, pp. 515–521, 2014.

[14] Z. Li, C. Yang, C.-Y. Su, S. Deng, F. Sun, and W. Zhang, "Decentralized fuzzy control of multiple cooperating robotic manipulators with impedance interaction," *IEEE Trans. Fuzzy Syst.*, vol. 23, no. 4, pp. 1044–1056, Aug. 2015.

[15] M. A. Llama, A. Flores, V. Santibáñez, and R. Campa, "Global convergence of a decentralized adaptive fuzzy control for the motion of robot manipulators: Application to the mitsubishi PA10-7CE as a case of study," *J. Intell. Robotic Syst.*, vol. 82, nos. 3–4, pp. 363–377, Jun. 2016.
[16] D. Shi, J. Zhang, Z. Sun, G. Shen, and Y. Xia, "Composite trajectory tracking control for robot manipulator with active disturbance rejection," *Control Eng. Pract.*, vol. 106, Jan. 2021, Art. no. 104670.
[17] D. Chen, "Active disturbance rejection control of indoor inspection robot in intelligent substation based on monocular vision," *J. Phys., Conf.*, vol. 1894, no. 1, Apr. 2021, Art. no. 012042.
[18] J. Gao, X. Liang, Y. Chen, L. Zhang, and S. Jia, "Hierarchical image-based visual serving of underwater vehicle manipulator systems based on model predictive control and active disturbance rejection control," *Ocean Eng.*, vol. 229, Jun. 2021, Art. no. 108814.
[19] D. Min, D. Huang, and H. Su, "High-precision tracking of cubic stewart platform using active disturbance rejection control," in *Proc. Chin. Control Conf. (CCC)*, Jul. 2019, pp. 3102–3107.
[20] J. Su, W. Qiu, H. Ma, and P.-Y. Woo, "Calibration-free robotic eye-hand coordination based on an auto disturbance-rejection controller," *IEEE Trans. Robot.*, vol. 20, no. 5, pp. 899–907, Oct. 2004.
[21] H. Yi, Z. Luo, M. Svinin, T. Odashima, and S. Hosoe, "Extended state observer based technique for control of robot systems," in *Proc. World Congr. Intell. Control Automat.*, vol. 4, 2002, pp. 2807–2811.
[22] C. Ren, Y. Ding, and S. Ma, "A structure-improved extended state observer based control with application to an omnidirectional mobile robot," *ISA Trans.*, vol. 101, pp. 335–345, Jun. 2020.
[23] B. Ding and Y. Li, "Hysteresis compensation and sliding mode control with perturbation estimation for piezoelectric actuators," *Micromachines*, vol. 9, no. 5, p. 241, May 2018.
[24] Y. Kali, M. Saad, K. Benjelloun, and M. Benbrahim, "Sliding mode with time delay control for robot manipulators," in *Proc. IEEE Int. Multidisciplinary Conf. Eng. Technol.*, Oct. 2017, pp 135–156.
[25] T. Van Tran, Y. Wang, H. Ao, and T. K. Truong, "Sliding mode control based on chemical reaction optimization and radial basis functional link net for de-icing robot manipulator," *J. Dyn. Syst., Meas., Control*, vol. 137, no. 5, May 2015, Art. no. 051009.
[26] S. Jung, "Improvement of tracking control of a sliding mode controller for robot manipulators by a neural network," *Int. J. Control, Autom. Syst.*, vol. 16, no. 2, pp. 937–943, Apr. 2018.
[27] Z. Wang, Y. Su, and L. Zhang, "A new nonsingular terminal sliding mode control for rigid spacecraft attitude tracking," *J. Dyn. Syst., Meas., Control*, vol. 140, no. 5, May 2018, Art. no. 051006.
[28] F. Zhang, "High-speed nonsingular terminal switched sliding mode control of robot manipulators," *IEEE/CAA J. Autom. Sinica*, vol. 4, no. 4, pp. 775–781, Dec. 2017.
[29] Z. Ma and G. Sun, "Dual terminal sliding mode control design for rigid robotic manipulator," *J. Franklin Inst.*, vol. 355, no. 18, pp. 9127–9149, 2017.
[30] Y. Yang, "A time-specified nonsingular terminal sliding mode control approach for trajectory tracking of robotic airships," *Nonlinear Dyn.*, vol. 92, no. 3, pp. 1359–1367, May 2018.
[31] A. Albu-Schaffer, C. Ott, and G. Hirzinger, "A unified passivity-based control framework for position, torque, and impedance control of flexible joint robots," *Int. J. Robot. Res.*, vol. 26, no. 1, pp. 23–39, 2007.
[32] G. Liu, S. Abdul, and A. A. Goldenberg, "Distributed control of modular and reconfigurable robot with torque sensing," *Robotica*, vol. 26, no. 1, pp. 75–84, Jan. 2008.
[33] B. Dong, T. An, F. Zhou, K. Liu, and Y. Li, "Decentralized robust zero-sum neuro-optimal control for modular robot manipulators in contact with uncertain environments: Theory and experimental verification," *Nonlinear Dyn.*, vol. 97, no. 1, pp. 503–524, Jul. 2019.
[34] L. Chen, M. Zhou, M. Wu, J. She, Z. Liu, F. Dong, and K. Hirota, "Three-layer weighted fuzzy support vector regression for emotional intention understanding in human–robot interaction," *IEEE Trans. Fuzzy Syst.*, vol. 26, no. 5, pp. 2524–2538, Oct. 2018.
[35] C. Mohiyeddini, R. Pauli, and S. Bauer, "The role of emotion in bridging the intention–behaviour gap: The case of sports participation," *Psychol. Sport Exercise*, vol. 10, no. 2, pp. 226–234, Feb. 2009.
[36] P. Wang, J. Liu, F. Hou, D. Chen, Z. Xia, and S. Guo, "Organization and understanding of a tactile information dataset TacAct for physical human-robot interaction," in *Proc. IEEE/RSJ Int. Conf. Intell. Robots Syst. (IROS)*, Sep. 2021, pp. 7328–7333.
[37] G. Liu, A. A. Goldenberg, and Y. Zhang, "Precise slow motion control of a direct-drive robot arm with velocity estimation and friction compensation," *Mechatronics*, vol. 14, no. 7, pp. 821–834, Sep. 2004.
[38] B. Dong, T. An, X. Zhu, Y. Li, and K. Liu, "Zero-sum game-based neuro-optimal control of modular robot manipulators with uncertain disturbance using critic only policy iteration," *Neurocomputing*, vol. 450, pp. 183–196, Aug. 2021.
[39] Q. Zheng, L. Q. Gaol, and Z. Gao, "On stability analysis of active disturbance rejection control for nonlinear time-varying plants with unknown dynamics," in *Proc. 46th IEEE Conf. Decis. Control*, 2007, pp. 3501–3506.
[40] B. Dong, T. An, F. Zhou, and W. Yu, "Model-free optimal decentralized sliding mode control for modular and reconfigurable robots based on adaptive dynamic programming," *Adv. Mech. Eng.*, vol. 11, no. 12, p. 1687814019896923, 2019.
[41] X. Zhu, B. Ma, B. Dong, K. Liu, and Y. Li, "Adaptive dynamic programming-based sliding mode optimal position-force control for reconfigurable manipulators with uncertain disturbance," in *Proc. Chin. Control Decis. Conf. (CCDC)*, Aug. 2020, pp. 421–427.
[42] B. Dong, T. An, F. Zhou, K. Liu, W. Yu, and Y. Li, "Actor-critic-identifier structure-based decentralized neuro-optimal control of modular robot manipulators with environmental collisions," *IEEE Access*, vol. 7, pp. 96148–96165, 2019.

XIAO PANG received the M.S. degree from the University of Nottingham, Ningbo, China, in 2014. She is currently a Lecturer with Changchun Guanghua University, China. Her research interests include machine learning and human emotion recognition.

XIAODONG MEN received the B.S. and M.S. degrees from the Changchun University of Technology, China, in 2018 and 2021, respectively. His research interests include robot control and active disturbance rejection control.

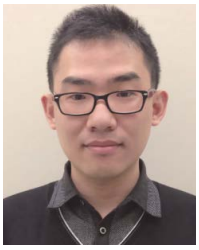

BO DONG received the M.S. and Ph.D. degrees from Jilin University, China, in 2012 and 2015, respectively. He is currently a Professor with the Changchun University of Technology, China. He is also a Postdoctoral Fellow with the State Key Laboratory of Management and Control for Complex Systems, Institute of Automation, Chinese Academy of Sciences, Beijing, China. His research interests include intelligent mechanical and robot control.

TIANJIAO AN (Student Member, IEEE) received the B.S. and M.S. degrees from the Changchun University of Technology, China, in 2017 and 2020, respectively, where he is currently pursuing the Ph.D. degree with the Department of Control Science and Engineering. His research interests include robot control and adaptive dynamic programming.